

## Vacuum tunneling spectroscopy of high-temperature superconductors: A critical study

P. Mallet, D. Roditchev, W. Sacks, D. Défourneau, and J. Klein

*Groupe de Physique des Solides, Universités Paris 6 and 7, Centre National de la Recherche Scientifique,  
2, pl. Jussieu, 75251 Paris, France*

(Received 6 June 1996)

Using scanning tunneling spectroscopy (STS) the local density of states (LDOS) of  $\text{Bi}_2\text{Sr}_2\text{Ca}_1\text{Cu}_2\text{O}_{8+\delta}$  [Bi(2212)] and  $\text{Y}_1\text{Ba}_2\text{Cu}_3\text{O}_{7-\delta}$  (YBaCuO) monocrystals were studied at low temperature (down to 4.2 K). Due to the high quality of the vacuum tunneling junctions the pair-breaking effects are consequently reduced, and rather fine features of the superconducting LDOS could be analyzed. For Bi(2212) it is shown that, in order to fit properly the experimental data,  $\mathbf{d}_{x^2-y^2}$  pairing (or a very anisotropic  $\mathbf{s}$  pairing) as well as a strong in-plane anisotropy of the Fermi surface are required. Although YBaCuO STS spectra look more “ $\mathbf{d}$  like,” no precise analysis was possible because of the high natural surface contamination of the samples. Both the fundamental problem of pairing symmetry and the influence of experimental conditions on vacuum STS measurements are discussed. [S0163-1829(96)08442-1]

### I. INTRODUCTION

Currently, the symmetry of the order parameter in high-temperature superconductors (HTSC's) is the subject of great interest. A considerable quantity of theoretical and experimental work is devoted to study the degree of anisotropy, by probing either the value or the phase of the energy gap (see Ref. 1). The number of review papers is growing<sup>1-5</sup> but, up to now, there is no consensus on the matter. Although a complex nonconventional character of the order parameter is quite established now, mechanisms responsible for HTSC's are still under discussion. In their pioneer works<sup>6,7</sup> Scalapino and co-workers suggested the dominant role of spin fluctuations in  $\mathbf{d}$  pairing. The detailed calculations of Monthoux *et al.*<sup>8</sup> clearly showed the possibility for  $\mathbf{d}$ -pairing symmetry in the presence of spin-fluctuation-induced interaction due to the strong antiferromagnetic correlations in copper oxides. In the recent paper of Combescot and Leyronas<sup>9</sup> the  $\mathbf{d}$  term occurs as the result of coupling between the Cu-O planes and the Cu-O chains. As a consequence, no  $\mathbf{d}$  pairing should exist in materials where there are no chains [as Bi(2212), for example]. Taking into consideration just the electron-phonon interaction in the presence of anisotropic in-plane Fermi surface originating from the Cu-O plane, also results in an anisotropic order parameter, without, however, phase reversal (anisotropic  $\mathbf{s}$  pairing).<sup>10</sup>

Tunneling spectroscopy (TS) was a key technique in the experimental proof of the BCS mechanism of conventional superconductivity. However, the TS results observed in HTSC's disagree significantly.<sup>5</sup> The origin of that is an extremely short coherence length and a high surface reactivity of HTSC's. Recently, some high-vacuum scanning tunneling spectroscopy (STS) experiments performed on *in situ* cleaved monocrystals have revealed more reproducible features of the local density of states (LDOS). Unfortunately, it was not sufficient to conclude definitively on the degree of pairing symmetry, since the theoretical curves for the DOS differ in finer details. The phase of the order parameter is much more sensitive to the pairing symmetry, but it cannot be studied within the STS technique alone. Recent, very

promising quantum interferometry experiments<sup>1,11</sup> have found some strong evidence for a  $\mathbf{d}$  pairing in HTSC's but, once more, there is a number of technical and experimental aspects which may influence the data.

In some papers<sup>12,13</sup> the quality of the tunneling junctions is analyzed using the criterion of whether or not the STS measurement may be successfully combined with the atomic resolution scanning tunneling microscope (STM) images. Others suggest however,<sup>14</sup> that the atomic resolution is neither necessary nor sufficient to obtain the “nonperturbed” LDOS spectra. In order to understand the variety of already published experimental results, we performed a systematic analysis of the parameters determining the junction quality, as well as the parasitic effects distorting the STS results.

### II. METHODS

Our variable temperature STM consists of two coaxial piezoelectric tubes (the tip translator and the sample one) glued to a Ti support. The choice of materials used is important to avoid thermal drift while cooling. The STM head is put in a vacuum can immersed into a standard He<sup>4</sup> cryostat. The temperature range of the STM in continuous operation is 2.5–100 K. However it is possible to operate our STM at any fixed temperature chosen between 100 and 350 K as well.

The details of the antivibration system as well as a specially developed tip approach, which are very important for STS measurements, are described elsewhere.<sup>15</sup> In the STS mode  $I_T(x_0, y_0, V_T)$  characteristics as well as ac lock-in assisted  $dI_T(V_T)/dV_T$  curves may be obtained. Since the lock-in technique requires a modulation signal of 1–2 mV in amplitude which may filter slightly the  $dI/dV$  curves, all data presented in this paper were taken directly in the form of  $I_T(x_0, y_0, V_T)$  scans and then differentiated numerically.

The measurements were performed on Bi(2212) and YBaCuO monocrystals using both Pt/Ir and Au tips. The Bi(2212) crystals were prepared using the self-flux method in an alumina crucible and then characterized.<sup>16</sup> The YBaCuO samples are fully oxygenated twinned single crystals. For the tip preparation both electrochemical and me-

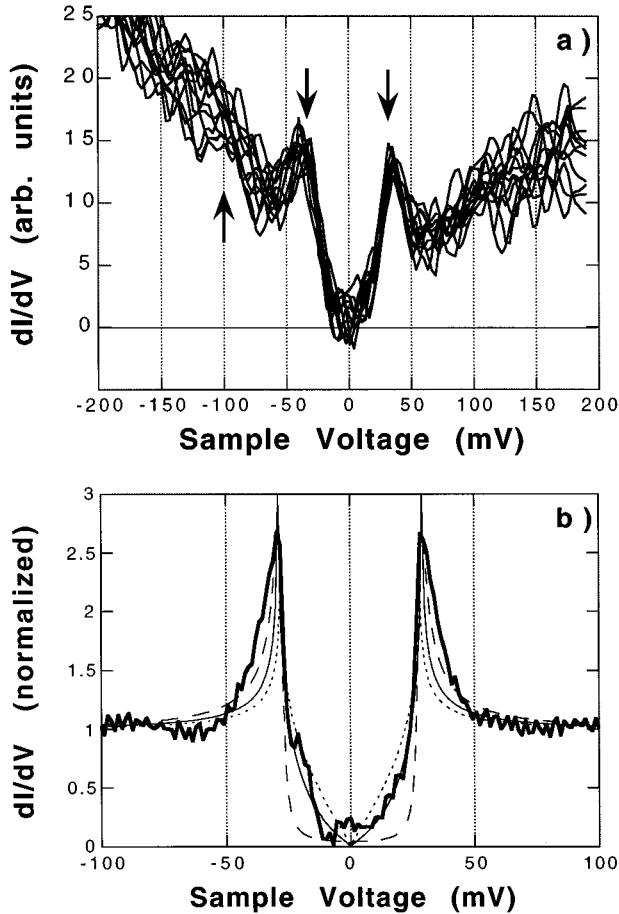


FIG. 1. Vacuum tunneling STS spectrum of Bi(2212) sample ( $T=4.2$  K): (a) spectra show almost no zero-bias states, two well pronounced maxima and weak  $dI/dV$  slope originating from the surface contamination. (b) corrected LDOS spectrum (thick solid line). Dashed line: the fit by the isotropic BCS curve ( $\Delta=28$  meV,  $T=4.2$  K,  $\Gamma=1.1$  meV); dotted line: the fit by a  $\mathbf{d}$ -wave model ( $\Delta_0=0$  meV,  $\Delta_1=28$  meV,  $T=4.2$  K,  $\Gamma=0$  meV); thin solid line:  $\mathbf{d}$  pairing in the presence of anisotropic in-plane Fermi surface ( $\gamma=0.5\pm 0.1$ ,  $\Delta_0=0$  meV,  $\Delta_1=28$  meV,  $T=4.2$  K,  $\Gamma=0$  meV).

chanical etchings were used. The samples were cleaved in air or in a pure  $\text{He}^4$  gas flow immediately before installing them into the can. The can was pumped and then filled at room temperature with pure  $\text{He}^4$  exchange gas at 200 mbars. Then, during the can cooling, the samples were continuously heated (up to 80 °C at the beginning) in order to favor the surface desorption.

### III. RESULTS AND EXPERIMENTAL CONDITIONS

A series of 16 consecutive STS curves obtained on the Bi(2212) sample with Pt/Ir tip at  $T=4.2$  K is shown in Fig. 1(a). The values  $V_T < 0$  corresponds to the occupied states, and  $V_T > 0$ , to the empty states of the sample. One sees the two peaks on both sides of the gap at the Fermi level to be well pronounced, the LDOS at the Fermi energy  $dI/dV(V_T=0)$  is as low as 5–10 % of the LDOS out of the gap. By comparison of corresponding areas in the  $dI/dV$  curve the total number of states in the peaks of the LDOS is found to be almost equal to that of “gapped” states. The form of the spectra does not depend on the tip-surface dis-

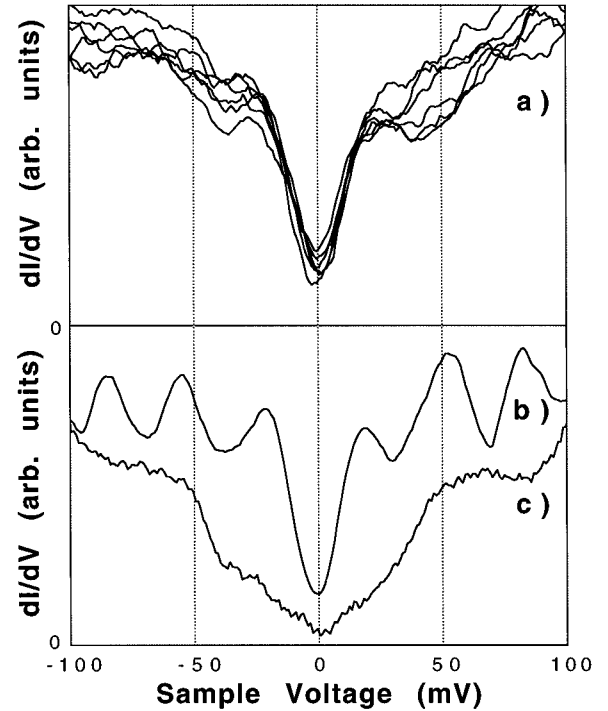


FIG. 2. STS spectra of YBaCuO sample ( $T=4.2$  K): (a) a series of “nonperturbed” STS spectra, taken at different lateral positions: two maxima on the both sides of the gap are seen. The zero-bias DOS is very important as compared to Bi(2212) (Fig. 1). (b) Coulomb staircase oscillations superpose the gap structure. (c) The spectrum is completely distorted by the Coulomb blockade.

tance. However, a slight rise of the conductivity out of the gap for both occupied states and empty states was often found. We believe this feature to come from the contribution of the surface conductivity and to be different from the bulk one. It seems that this channel of current leakage does not reflect intrinsic properties of the material. Thus, some correction procedure is required in order to extract the real LDOS of the sample. The corrected spectrum is presented in Fig. 1(b) (the details of data reduction are treated in the Sec. IV). The spectra are reproducible laterally over a typical area of 200–500 Å in radius. We suppose this value to be characteristic for the size of superconducting zones on the sample surface.

Characteristic YBaCuO  $dI/dV$  spectra taken at different points of the sample surface are presented in Fig. 2(a). With respect to the Bi(2212) spectrum, the curves show a large offset. The U-shaped wings are more important, the maxima at  $\pm\Delta$  are strongly damped, and the total number of states is not conserved. The general shape of the spectrum is similar to that observed in planar junction experiments,<sup>17</sup> as well as in recent vacuum STS measurements.<sup>18</sup> However, the fine zero-bias structure reported in these papers was not reproducibly seen.

Before attributing fine characteristics of the spectra to a particular pairing symmetry, it is necessary to detail some aspects which may influence the experimental data.

*Surface contamination.* Surface reactivity plays an important role in both compounds: once cleaved in air the surface is almost instantaneously contaminated by adsorbates. The

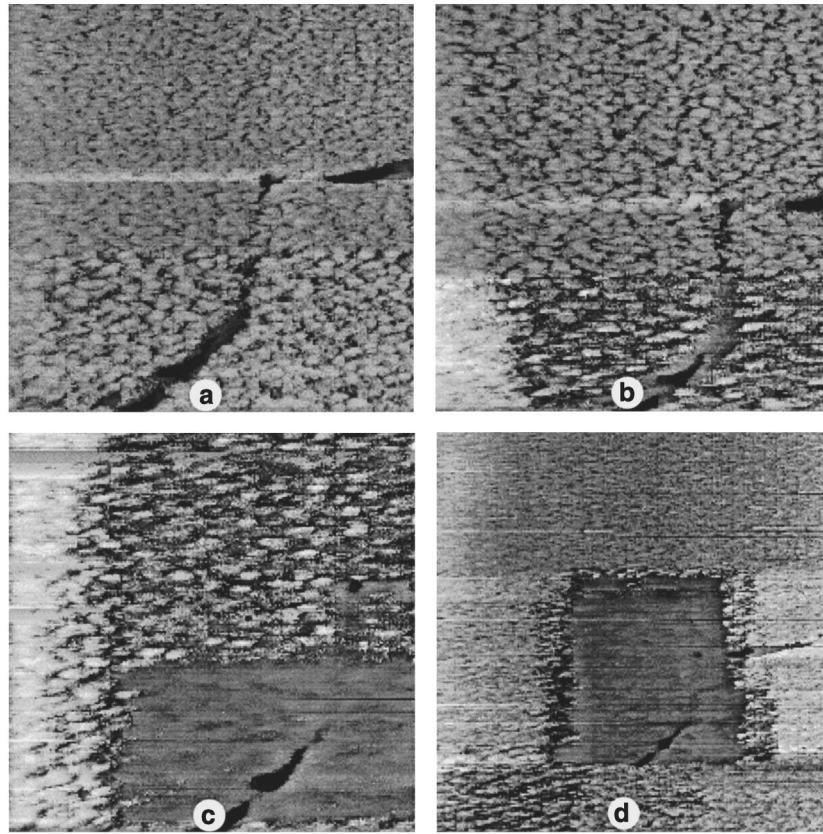


FIG. 3. (a)–(c)  $1\ \mu\text{m}\times 1\ \mu\text{m}$  and (d)  $2\ \mu\text{m}\times 2\ \mu\text{m}$  consecutive STM images of the same surface of Bi(2212) ( $T=300\ \text{K}$ , Pt/Ir tip,  $V_{\text{sample}}=-100\ \text{mV}$ ,  $I=0.5\ \text{nA}$ ): (a) first scan image; (b) third scan image; (c) fifth scan image; (d) surface is “cleaned”: no more clusters left in the scanned area.

surface electronic states are modified, and the upper layer may have a very different DOS from that in the bulk material (we find either semimetallic, semiconducting or even insulating zones). This naturally contaminated layer strongly modifies the STS data, since the STM probes electronic states at the immediate surface layer.

*Oxygen content.* The Cu-O plane is believed to be responsible for the conductivity in the HTSC's. The superconducting properties are known to be very sensitive to the oxygen content in these layers. For the optimum structures (the higher  $T_c$  values) the oxygen density is out of stoichiometry equilibrium. The interaction between mobile oxygen atoms from the Cu-O layers just underlying topmost Bi-O layer, and the multiple surface imperfections (point defects, atomic steps, dislocations, and interfaces between twins) result in the oxygen content modification near the sample surface. This is an important argument to be considered in STS data analysis: to avoid a modification in oxygen content in the junction region, an atomically perfect surface should be obtained on the area of the order of the in-plane oxygen diffusion length squared [i.e., about  $(0.1\text{--}1.0\ \mu\text{m})^2$  for a sample cleaved in air, which is rather difficult to achieve].

*Surface conductivity.* The surface states result in a number of features perturbing the intrinsic STS curves. One can distinguish two different mechanisms: surface conductivity versus bulk conductivity and charging/recharging effects.

The surface DOS modifications due to the variation of the O content and (or) adsorbate-induced DOS modifications lead to an additional series-to-parallel channel of tunnel cur-

rent. If the number of surface states with respect to the bulk ones is reduced (semiconducting or insulating surface states) the surface plays a role of an additional, bias-dependent potential barrier *in series* with the vacuum one. If the surface contamination leads to a rise in the number of the surface states, the surface leakage current will result in a *parallel* current channel.

These features are clearly seen on many  $dI/dV$  STS results. In the first case, the intrinsic DOS curve is distorted by a V-shaped form coming from the bias-induced barrier damping. In the second one, a parallel conductivity (usually a non-Ohmic, hoppinglike one) results in an offset in the density of states in addition to the superconducting DOS. One may see a complex combination of both effects on many STS results on HTSC's published before 1993 (see Ref. 5 for a review).

*Semi-insulating clusters.* When STM topographic experiments are performed on the **ab** surface of Bi(2212) at room temperature, in an atmosphere of  $\text{He}^4$  gas, some clusters  $100\text{--}300\ \text{\AA}$  in size are seen [Fig. 3(a)]. The high-resolution STM shows that the cluster's atomic structure is quite similar to the one expected for the **ab** plane of Bi(2212). The size and position of the clusters change progressively due to the tip-sample interaction as consecutive scans are performed [Figs. 3(b) and 3(c)]. The result of this surface “cleaning” after six scans is shown in Fig. 3(d): the scanned surface (in the center of the image) is much more regular; atomic resolution images on the cleaned area may be also reached. However, the STS measurements performed on the clusters show

a non-Ohmic U-like LDOS. The DOS at the Fermi energy  $dI/dV(0)$  is rather low and seems to be thermally activated. We stress that, in this experiment, the tunnel resistance was  $R_T=200$  M $\Omega$ . As we show later, even at this rather high value of  $R_T$ , the tip-surface distance is too small to probe the intrinsic superconductor LDOS of the sample. Probably, the high surface reactivity of HTSC's leads to the formation of these small clusters of different oxygen content (with respect to the bulk material). As a consequence, a different and generally more "insulating" LDOS is observed.

These clusters seem to be the culprit for charging effects which are well-known in tunneling spectroscopy. The tunnel current is strongly influenced by the capacitive part of the tunnel impedance and hence the STS data are perturbed. The first effect, the Coulomb blockade, comes from the fact that the cluster, weakly coupled to underlying metallic layers as well as to the tip, form a capacitor of small capacitance  $C$ . In a capacitor, a portion of energy  $\sim e^2/2C$  should be attributed to transfer a carrier of charge  $e$  from one electrode to another. At  $T=0$  K and at low biases, the energy transmitted from the battery to a carrier  $\sim eV_T$  is not high enough with respect to  $e^2/2C$ , and tunneling is not possible. For biases larger than the threshold  $e/2C$ , the carrier may be transferred across the junction. On the STS data, this means that the  $I(V)$  curve extrapolated from the region of positive (or negative) biases to the origin does not pass through point  $I=0$ ,  $V=0$  but through  $I=0$ ,  $V=e/2C$  (or through  $I=0$ ,  $V=-e/2C$ , respectively).<sup>19</sup> Thus, at low temperature  $T \leq e^2/2kC$  the Coulomb blockade manifests itself as a gap structure smoothed by  $kT$  which appears around zero bias on the both sides of the  $dI/dV$  curve [Fig. 2(c)].

The second effect, the Coulomb staircase, is well-known in granular structures<sup>19,20</sup> where tunneling occurs through many capacitive junctions (generally two are necessary to explain the effect). A series of oscillations superposes the  $dI/dV$  STS curve in this case [Fig. 2(b)].

*Tip-sample separation and tunneling resistance.* In the STM topographic mode, the experiments are usually done choosing low tunnel resistance values: typically 10–100 mV bias is applied, and the tunnel current of  $10^{-9}$  A flows across the junction. This is equivalent to  $R_T=10$ –100 M $\Omega$ . The main reason for this choice is related to the exponential damping of the carrier wave function in the  $z$  direction. To obtain an atomic resolution image one places the tip as close as possible to the sample surface in order to have a sufficient tunnel current contrast and to not lose the atomic pattern information. In most cases, the tip-surface separation should be typically of the same order of magnitude as a lattice constant of the sample studied. This leads to a strong tip-surface interaction, resulting in uncontrolled changes of the tip LDOS and/or tip contamination by surface atoms. As a consequence, one often finds image contrast variations, giant corrugations, etc. Since the tunnel current is a convolution of both the tip and the surface electronic states, any singularities appearing in the tip electronic structure perturb the STS data.

The slope  $d \ln z(V)/dV$  measured in Bi(2212) at  $R_T \leq 100$  M $\Omega$  is found to be much larger than that for  $R_T \geq 1$  G $\Omega$ . Thus, at these "small"  $R_T$  values the sample surface becomes more "elastic." Taking into account the contribution of surface conductivity to the total current, we suggest that

the tip presses onto the surface, and the resulting current reflects more the point contact regime, with its characteristic nonlinear conductivity [known as a V shape in  $dI(V)/dV$ ] rather than the vacuum tunneling process. The tip also applies a high local pressure perturbing the LDOS of the sample in the contact area. The gap value measured in this kind of experiments, as well as the general form of  $I(V)$  and  $dI(V)/dV$  curves, depend on the  $R_T$  value, which should not be the case for real vacuum tunneling. That is why we suggest *the uniformity of the spectrum shape on the tip-sample distance* to be an important condition for correct STS measurements. Since this requires rather high tip-surface separation, no atomic resolution could be achieved in such a case. For instance, in our experiments this condition was acquired at  $R_T \geq 1$  G $\Omega$  (typically  $V_T=250$ –800 mV,  $I_T=50$ –200 pA). Moreover, in most cases we avoided the combination of the STM and the STS measurements in the same series of experiments in order to avoid tip contamination. In all stages of our STS experiments, the tunnel resistance was maintained at values higher than 1 G $\Omega$ .

#### IV. DATA ANALYSIS

The initial step in the data analysis is to subtract the background conductivity from  $dI/dV$  spectra. Since the experiment is carried out at high tunneling resistances, the point-contact regime with its characteristic V-shape background is not expected. However, a nonlinear conductivity may come from the surface states due to Bi-O topmost layer contamination as it is discussed above. In this case the tunneling current is affected by leakage currents through the clusters, and a parabolic increasing of the background conductance near Fermi level  $E_F$  is dominant. This unusual smeared gaplike feature at  $E_F$  was observed in Ref. 14. Thus, in order to extract intrinsic superconducting features we subtract a parabolic function from the initial  $dI/dV$  spectrum. This function does not consist of any free term, so no correction is done near  $V=0$ . The curves are then normalized to have the value about unity rather far from the gap (at  $-100$  meV). The corrected LDOS is presented in Fig. 1(b) as a solid line. It is important to note a high amplitude of the peaks at  $V=\pm 29$  mV (2.7 for the normalized curve) which is a proof for a high-quality tunneling junction. The spectra are nearly identical to the LDOS observed on a sample cleaved *in situ* ultrahigh vacuum.<sup>14</sup>

In metal-vacuum-superconductor TS measurements, the  $dI(V)/dV$  curves are usually fitted using the BCS model (corresponding to isotropic s pairing):

$$\frac{dI}{dV} \propto \int_{-\infty}^{+\infty} dE N_S(E) \left\{ - \frac{\partial f(E-eV)}{\partial V} \right\}, \quad (1)$$

where the density of states of the metallic electrode near the Fermi level is considered to be constant,  $N_S(E)$  is the tunneling superconducting density of states:

$$N_S(E) = N_N(0) \frac{E}{\sqrt{E^2 - \Delta^2}}, \quad E > \Delta$$

$$N_S(E) = 0, \quad E < \Delta, \quad (2)$$

$f(E)$  is the Fermi-Dirac distribution and  $N_N(0)$  is the normal density of states at the Fermi level. The function  $(\partial/\partial V)f(E - eV)$  is sharply peaked at  $E = eV$ , with a width about  $4kT \approx 1$  meV at 4.2 K.

In order to explain an important broadening of the experimental spectra, which is usually found to be higher than the thermal one, some authors invoke a finite lifetime of quasiparticles in the tunneling process by replacing  $E$  by  $E - i\Gamma$ , where  $\Gamma$  is a phenomenological pair-breaking parameter. This consideration permits a better fit to the tunneling spectra but unfortunately results in the loss of information on the symmetry of the order parameter. A high amplitude of the maxima of spectra observed in this work gives a fit to the data with a rather small pair-breaking parameter  $\Gamma \leq 1$  meV. This fact is of great importance: if  $\Gamma$  is higher than 2–4 meV, the fine features of the LDOS are attenuated and the fitting procedure becomes almost independent of the degree of anisotropy of the order parameter.

The best fit by the BCS curve ( $\Delta = 28$  meV,  $\Gamma = 1.1$  meV,  $T = 4.2$  K) is presented as the dashed line in Fig. 1(b). The value of  $\Delta$  is in a good agreement with recent results.<sup>14</sup> The BCS expression fits well the maxima and the tails of the experimental curve but not the LDOS within the gap. It is not surprising, since Eq. (2) is only justified for a BCS-type superconductor, with an isotropic Fermi surface. In the case of HTSC's, a strong anisotropy of the order parameter may occur. Since the tunneling experiment is not sensitive to the phase of the order parameter, we choose, as a first approximation:

$$\Delta^2(\varphi) = \Delta_0^2 + \Delta_1^2 \cos^2(2\varphi), \quad (3)$$

where  $\varphi$  is the polar angle in  $\mathbf{k}_{ab}$  space. The values of  $\Delta_0$  and  $\Delta_1$  are the s term and the anisotropic term, respectively, and the ratio  $\Delta_1/\Delta_0$  gives the degree of anisotropy. Tunneling with an axially symmetric tip requires integration over  $\varphi$ :

$$N_S(E) = N_N(0) \frac{1}{2\pi} \int \operatorname{Re} \left[ \frac{E}{\sqrt{E^2 - \Delta(\varphi)^2}} \right] d\varphi. \quad (4)$$

The dotted line in Fig. 1(b) is the best fit for **d**-wave pairing [ $N_S(E)$  is taken from Eq. (4) with  $\Delta(\varphi)$  given by Eq. (3)]. The fit parameters are  $\Delta_0 = 0$  meV,  $\Delta_1 = 28$  meV,  $T = 4.2$  K,  $\Gamma = 0$  meV. Although this model gives a higher density of states inside the gap, it does not fit better the general shape of the LDOS: the maxima on the theoretical curve, calculated for  $T = 4.2$  K without any pair-breaking parameter, are less pronounced than the maxima on the experimental one. Even more general anisotropic **s** or **s+d** expressions ( $\Delta_0 \neq 0$ ,  $\Delta_1 \neq 0$ ) are not much more successful. However, we could estimate the upper limit for  $\Delta_0 \leq 6$ –10 meV, whereas  $\Delta_1$  was found to be 25–32 meV.

To calculate more precisely  $N_S(E)$ , one must take into account the particularities of the two-dimensional Fermi surface of Bi(2212). Indeed, due to the strong anisotropy of the material, one can consider that the essential features of the electronic structure near  $E_F$  to be due to the Cu-O plane. The Cu-O square lattice leads to an anisotropic Fermi surface of fourfold symmetry, and in the half-filled band approximation even the van Hove singularities may lie at the Fermi level.<sup>21</sup>

The normal density of states at the Fermi level is an integral over the contour  $l_{\mathbf{k}}(0)$  of constant energy  $E(\mathbf{k}) = 0$ :

$$N_N(0) = \oint_{l_{\mathbf{k}}(0)} \frac{dl_{\mathbf{k}}(0)}{|\nabla_{\mathbf{k}} E|_{E=0}}. \quad (5)$$

It is easy to show that in polar coordinates  $\mathbf{k}_{ab} = (k, \varphi)$ , this expression can be rewritten as following:

$$N_N(0) = \frac{1}{2\pi} \int_0^{2\pi} n_N(0, \varphi) d\varphi, \quad (6)$$

where we introduce  $n_N(0, \varphi) d\varphi$ , the number of states at the Fermi level in the direction given by  $\varphi$ .

The anisotropic Fermi surface further modifies the superconducting density of states. Indeed, using Eqs. (2) and (6) we obtain

$$N_S(E) = \frac{1}{2\pi} \int_0^{2\pi} n_S(E, \varphi) d\varphi, \quad (7)$$

with

$$n_S(E, \varphi) = n_N(0, \varphi) \operatorname{Re} \left[ \frac{E}{\sqrt{E^2 - \Delta^2(\varphi)}} \right]. \quad (8)$$

To enhance the LDOS fit we have to suppose  $n_N(0, \varphi)$  to be anisotropic with the maxima along the same directions as the maxima of the order parameter. As a first approximation we suppose

$$n_N(0, \varphi) = n_0 + n_1 \cos(4\varphi) = n_0 [1 + \gamma \cos(4\varphi)], \quad (9)$$

where  $\gamma = n_1/n_0$ . The best fit [thin solid line in Fig. 1(b)] corresponds to  $\gamma = 0.5 \pm 0.1$ ,  $\Delta_0 = 0$  meV,  $\Delta_1 = 29$  meV,  $T = 4.2$  K,  $\Gamma = 0$  meV [here  $N_S(E)$  is given by Eqs. (7)–(9) with  $\Delta(\varphi)$  from Eq. (3)]. Because of the limiting signal-to-noise ratio we are not able to evaluate the value of  $\gamma$  with a better accuracy. Here it is important to note, that no pair-breaking parameter was needed to fit the data. A slightly higher amplitude of the peaks on the theoretical curve with respect to the experimental one is naturally explained by the limiting pass band of our data acquisition system.

The  $dI/dV$  curves obtained in YBaCuO [see Fig. 2(a)] were not fitted because of their strong distortion by the parasitic effects described above, high pair-breaking and strong zero-bias conductivity. We believe these effects to originate from the surface states due to a higher reactivity of the surface of YBaCuO with respect to Bi(2212). However, taking into account similar results,<sup>17,18</sup> one may find our curves more **d** shaped.

## V. CONCLUSIONS

In this paper we tried to analyze critically the low-temperature STS data obtained on BiSrCaCuO and YBaCuO monocrystals. Both the fundamental problem of pairing symmetry and experimental aspects of vacuum tunneling STS measurement were discussed.

For BiSrCaCuO directly obtained  $dI/dV$  curves show a gap structure in the LDOS with no states (less than 5–10 %) at the Fermi level followed by well-pronounced maxima. The maxima have the same total area as the gapped states, so

the total number of states is conserved. However, the original  $dI/dV$  curves have a slight nonconstant U-like term which comes from surface states. This term was subtracted out before performing the fitting procedure. The spectra corrected in this way were found to be similar to those observed by Renner and Fisher.<sup>14</sup> Precise analysis of the  $dI/dV(V)$  STS spectra clearly show that neither isotropic  $s$  pairing nor pure  $d_{x^2-y^2}$  pairing fit properly the experimental data if the in-plane Fermi surface is taken to be isotropic. In the presence of the anisotropic Fermi surface of fourfold symmetry, either very anisotropic  $s$ -state ( $\Delta_0 \leq 6-10$  meV,  $\Delta_1 = 25-32$  meV) or  $d$ -state models are required to explain the results. Although YBaCuO STS spectra look more  $d$  like, no fitting was done for YBaCuO STS data, since, due to high distortion of the spectra by number of parasitic effects, the subtraction procedure becomes uncertain for energies within the gap.

It is shown that, in order to avoid a number of parasitic effects in STS, some experimental conditions are required. These conditions come directly from the natural properties of the HTSC surface. Reproducible spectra may be observed even without *in situ* cleavage. However in the case of air-cleaved samples, the surface states slightly distort the real LDOS, and an additional correction procedure is necessary before studying the LDOS fine structure.

#### ACKNOWLEDGMENTS

We thank Ch. Simon and V. Hardy for providing the Bi(2212) single crystals, and K. Behnia for the YBaCuO single crystals. We are also grateful to Professor J. Bok for many stimulating discussions.

- 
- <sup>1</sup>D. J. V. Harlingen, *Rev. Mod. Phys.* **67**, 515 (1995).  
<sup>2</sup>J. R. Schrieffer, *Solid State Commun.* **92**, 129 (1994).  
<sup>3</sup>R. C. Dynes, *Solid State Commun.* **92**, 53 (1994).  
<sup>4</sup>D. Pines, *High- $T_c$  Superconductivity and the C60 Family* (Gordon and Breach, New York, 1995).  
<sup>5</sup>K. Kitazawa, *Science* **271**, 313 (1996).  
<sup>6</sup>N. E. Bickers, D. J. Scalapino, and R. T. Scalettar, *Int. J. Mod. Phys. B* **1**, 687 (1987).  
<sup>7</sup>N. E. Bickers, D. J. Scalapino, and R. White, *Phys. Rev. Lett.* **62**, 961 (1989).  
<sup>8</sup>P. Monthoux, A. V. Balatsky, and D. Pines, *Phys. Rev. B* **46**, 14 803 (1992).  
<sup>9</sup>R. Combescot and X. Leyronas, *Phys. Rev. Lett.* **75**, 3732 (1995).  
<sup>10</sup>J. Labbé and J. Bok, *Europhys. Lett.* **3**, 1225 (1987).  
<sup>11</sup>C. C. Tsuei *et al.*, *Science* **271**, 329 (1996).  
<sup>12</sup>T. Hasegawa, M. Nantoh, and K. Kitazawa, *Jpn. J. Appl. Phys.* **30**, L276 (1991).  
<sup>13</sup>H. L. Edwards, J. T. Markert, and A. L. d. Lozanne, *Phys. Rev. Lett.* **69**, 2967 (1992).  
<sup>14</sup>Ch. Renner and Q. Fisher, *Phys. Rev. B* **51**, 9208 (1995).  
<sup>15</sup>P. Mallet *et al.*, *J. Vac. Sci. Technol. B* **14**(2) (1996).  
<sup>16</sup>A. Ruyter *et al.*, *Physica C* **225**, 235 (1994).  
<sup>17</sup>J. M. Valles, Jr. *et al.*, *Phys. Rev. B* **44**, 11 986 (1991).  
<sup>18</sup>I. Maggio-Aprile *et al.*, *Phys. Rev. Lett.* **75**, 2754 (1995).  
<sup>19</sup>H. v. Kempen, in *Scanning Tunneling Microscopy and Related Methods*, edited by R. J. Behm, N. Garcia, and H. Rohrer (Kluwer, Dordrecht, 1990), p. 241–267.  
<sup>20</sup>P. J. M. v. Bentum, R. T. M. Smokers, and H. v. Kempen, *Phys. Rev. Lett.* **60**, 2543 (1988).  
<sup>21</sup>J. Bouvier and J. Bok, *Physica C* **249**, 117 (1995).